ISOTOPIC STUDIES OF EPIGENETIC FEATURES IN METALLIFEROUS SEDIMENT, ATLANTIS II DEEP, RED SEA

ROBERT A. ZIERENBERG

U.S. Geological Survey, MS 901, 345 Middlefield Road, Menlo Park, California 94025, U.S.A.

WAYNE C. SHANKS, III

U.S. Geological Survey, MS 954, National Center, Reston, Virginia 22092, U.S.A.

ABSTRACT

The unique depositional environment of the Atlantis II Deep brine pool, in the Red Sea, produces a stratiform metalliferous deposit of much greater areal extent than deposits formed by buoyant-plume systems typical of the midocean ridges because of much more efficient metal entrapment. Isotopic analyses of strontium, sulfur, carbon, and oxygen from the metalliferous sediments indicate that three major sources contribute dissolved components to the hydrothermal system: seawater, Miocene evaporites, and rift-zone basalt. Incoming hydrothermal fluid with a temperature >250°C brings sulfide with $\delta^{34}S \approx 5\permil$ and dissolved metals into the brine pool. Mixing of the hydrothermal fluid with cooler sulfate-bearing brine causes precipitation of sulfides and sulfates that are not in chemical or isotopic equilibrium. The $\delta^{34}S$ and $\delta^{18}O$ values of sulfate minerals range from those of epigenetic veins, with values typical of the present-day lower brine mass, to those of brine-pool precipitates, with values similar to Miocene evaporites recovered from DSDP 227. The values of $\delta^{18}O$ from dissolved sulfate in the brine and sulfate minerals in epigenetic veins reflect the high-temperature origin of the hydrothermal fluid. The range of isotopic values suggests mixing of isotopically distinct fluids. Carbonate in the metalliferous sediment has two sources: biogenic carbonate precipitated in normal Red Sea water at 19°C, and hydrothermal carbonate precipitated in the lower brine at temperatures of 47 to 82°C. Smectite in metalliferous sediments precipitated within the brine pool at temperatures of 57 to 110°C (the present-day brine temperature is 62.3°C). Smectite in epigenetic veins precipitated from incoming hydrothermal fluid over a temperature range of 145 to 270°C. An areally restricted magnetite–hematite–pyroxene assemblage formed at high temperatures, possibly in response to hydrothermal convection initiated by intrusion of basalt into the metalliferous sediment. A correlation between smectite Fe/(Fe + Mg) ratios and oxygen isotope temperatures suggests that smectite is a potentially important chemical geothermometer, and confirms geochemical calculations indicating that Mg-rich smectite is more stable than Fe-rich smectite at elevated temperatures.

Keywords: Atlantis II Deep, metalliferous sediment, massive sulfide, brine pool, stable isotopes, strontium isotopes, smectite, geothermometry, seawater–rock interaction, fluid mixing, Red Sea.

SOMMAIRE

L'unique milieu dépositionnel du bassin de saumures
dans l'abysse de Atlantis II (mer Rouge) a donné un gisement métallifère stratiforme d'une étendue beaucoup plus grande que les dépôts produits par les panaches typiques des dorsales médio-océaniques, à cause d'une concentration beaucoup plus efficace de métaux. Les mesures isotopiques de strontium, de soufre, de carbone et d'oxygène des sédiments métallifères montrent que trois sources de constituants dissous sont importants dans le système hydrothermal: l'eau de mer, les évaporites miocènes, et les basaltes du rift. Le fluide hydrothermal, introduit dans le bassin de saumures à une température supérieure à 250°C, apporte le sulfure, qui possède une valeur $\delta^{34}S$ de 5‰, environ. Le mélange de ce fluide avec les saumures, moins chaudes et porteuses de sulfate, cause une précipitation des sulfures et des sulfates, qui ne sont pas en équilibre, ni chimique, ni isotopique. Les indices $\delta^{34}S$ et $\delta^{18}O$ des minéraux sulfatés ont des valeurs entre celles typiques des sulfates des fissures épigénétiques ainsi que de la masse inférieure des saumures modernes, et celles des précipités des bassins de saumures, qui ressemblent aux valeurs des évaporites miocènes, échantillonnées dans le forage DSDP 227. Les valeurs de $\delta^{18}O$ des sulfates dissous dans les saumures et cristallisés dans les fissures épigénétiques reflètent l'origine du fluide hydrothermal à haute température. La diversité des valeurs isotopiques résulterait d'un mélange de fluides isotopiquement distincts. Le carbonate dans les sédiments métallifères provient de deux sources; le carbonate biogénique cristallise dans l'eau de la mer Rouge, à 19°C, tandis que le carbonate hydrothermal est formé dans les profondeurs du bassin de saumures, entre 47 et 82°C. La smectite des sédiments métallifères du bassin a cristallisé entre 57 et 110°C (la température des saumures modernes est de 62.3°C). La smectite des fissures épigénétiques a été formé entre 145 et 270°C à partir du fluide hydrothermal introduit. Un assemmblage magnétite — hématite — pyroxène d'importance locale a été formé à haute température, peut-être comme résultat d'une cellule de convection hydrothermale initiée par l'intrusion d'un magma basaltique dans le sédiment métallifère. Une corrélation entre les valeurs de Fe/(Fe + Mg) de la smectite et la température indiquée par les isotopes d'oxygène montre que la smectite constitue un géothermomètre potentiellement important, et confirme les calculs géochimiques qui prédisaient une smectite magnésienne plus stable qu'une smectite ferrifère à température élevée.

(Traduit par la Rédaction)

Mots-clés: abysse de Atlantis II, sédiment métallifère, sulfure massif, bassin de saumures, isotopes stables, isotopes strontium, smectite, géothermométrie, interaction roche — eau de mer, mélange de fluides, mer Rouge.

INTRODUCTION

Studies of hydrothermal activity and sulfide deposition along midocean ridges have provided insight into the geochemistry of ore-forming systems. The first actively forming deposit of seafloor sulfides was discovered underlying metal-rich brine in the Atlantis II Deep in the axial rift zone of the Red Sea (Degens & Ross 1969) (Fig. 1). This segment of the Red Sea is a slow spreading center with a total opening rate of 1.5 cm/y (Roeser 1975).

The Atlantis II deposit remains the largest sulfide accumulation discovered on the seafloor. It contains ≈227 mt of metalliferous sediment (Bäcker 1976),

90 mt of which have a grade of 2.06% Zn, 0.45% Cu and 38.4 g/t Ag (Nawab 1984). This hydrothermal deposit, which has formed within the last 15,000 years (Shanks & Bischoff 1980), is comparable in magnitude to the largest known volcanogenic massive sulfide deposits on land.

The importance of a brine pool in the formation of large stratiform sulfide deposits is well-illustrated by a comparison of open-ocean ridge-crest deposits with the restricted brine-pool setting of the Atlantis II deposit (Zierenberg 1984). The metalliferous sediments of the Atlantis II Deep are fine-grained, delicately laminated silicates, sulfides, and oxides that settled slowly from superjacent brine layers (Bischoff
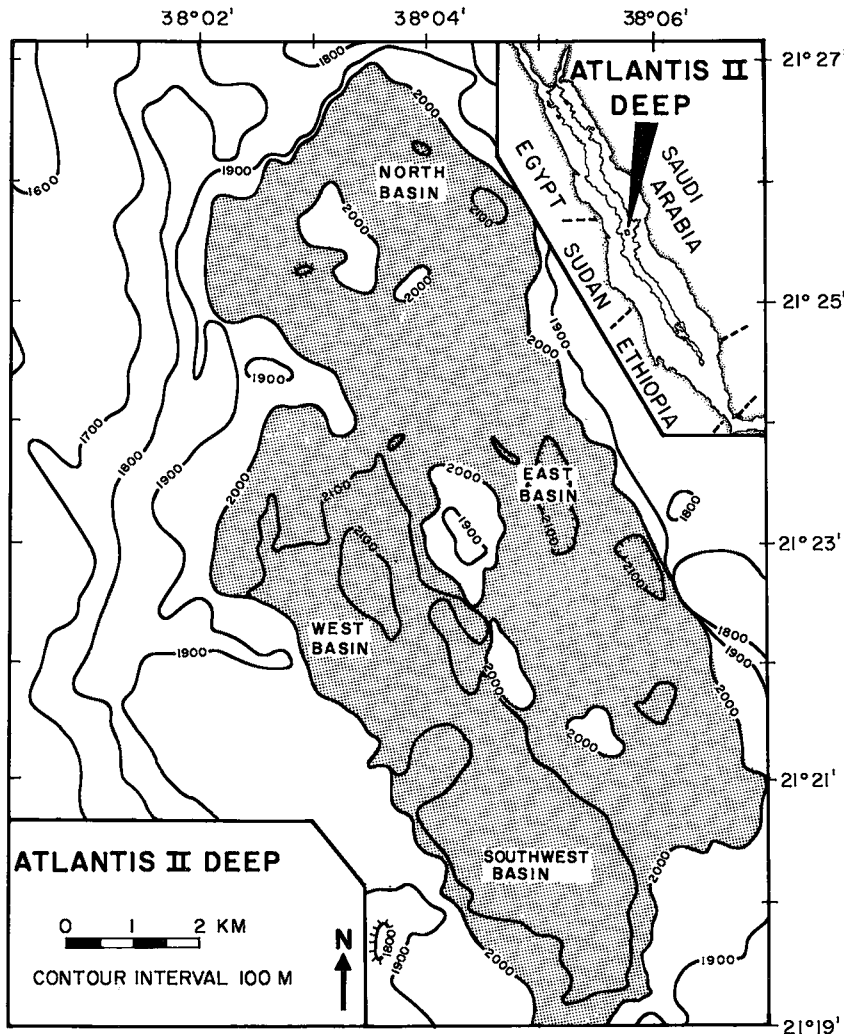

FIG. 1. Inset map shows the location of the Atlantis II Deep in the central Red Sea; the 500-m contour defines the main trough of the Red Sea. The bathymetric map of the Atlantis II Deep graben shows the location of the different basins. The patterned area below approximately 2000 m is covered by brine.

1969, Bäcker & Richter 1973, Zierenberg & Shanks 1983). The sediments differ substantially from the small, consolidated mounds and chimneys developed along open-ocean spreading centers, as exemplified by volcanic-hosted deposits on the East Pacific Rise (EPR) at 21°N (Haymon & Kastner 1981, Goldfarb *et al.* 1983) and on the Juan de Fuca Ridge (Koski *et al.* 1984, Tivey & Delaney 1986). However, recent studies have revealed many similarities, including evolved-seawater hydrothermal fluids, 350°C phase equilibria, low-fS_2 primary sulfide assemblages (Pottorf & Barnes 1983, Schumann 1978), and isotopic evidence indicating basalt–seawater interaction (Delevaux & Doe 1974, Faure & Jones 1969, Lupton *et al.* 1977, Zierenberg & Shanks 1986). Sulfide assemblages in both settings are rich in zinc and copper, but poor in lead, which is consistent with a basaltic source for much of the metal.

Venting of low-salinity, 350°C hydrothermal fluid onto the seafloor, *e.g.* at 21°N EPR, leads to the formation of small, high-grade sulfide–sulfate deposits around the immediate sites of venting. Most of the dissolved load of the hydrothermal fluid is carried away from the site of sulfide deposition by buoyant hydrothermal plumes and is dispersed over a large depositional area (Fig. 2). When venting stops, sulfide deposits are immediately subjected to dissolution and oxidation by ambient seawater.

In contrast, venting of a high-salinity hydrothermal fluid into a seafloor depression generally results in development of a submarine brine pool (Fig. 2) because of the high rate of diffusion of heat relative to that of dissolved components (Sato 1972, McDougall 1984a,b). In the Atlantis II Deep, confinement of the hydrothermal fluid to the anoxic lower brine leads to efficient deposition of sulfidic sediments over an area that is large (≈ 40 km^2), but is contained. Little of the dissolved metal load is dispersed beyond the Atlantis II Deep (Bignell *et al.* 1976). However, because of the coprecipitation of iron silicates and oxides, the economically important metal sulfides are diluted and have lower metal grades than deposits of buoyant-plume systems formed in open ocean settings. Moreover, reactions resulting from fluid advection or diffusive mixing across brine boundaries (Fig. 3) cause geochemical fractionation of elements such as iron and manganese, and produce distinct facies patterns in the metalliferous deposits (Bischoff 1969, Hartmann 1973, Bäcker & Richter 1973). Mixtures of facies can result either from cosedimentation or resedimentation of minerals initially precipitated within different geochemical environments of the stratified brine pool (Fig. 3).

Critical information that can be obtained at open-ocean ridge systems by direct sampling of vent fluid with submersibles is precluded by the high density and inhospitable nature of the pools (Monin *et al.* 1981, 1982). Therefore, we must rely on indirect evidence about the nature of the hydrothermal fluid in brine pools, such as the mineralogical record preserved in the metalliferous sediments. In the Atlantis II Deep, information about the hydrother-
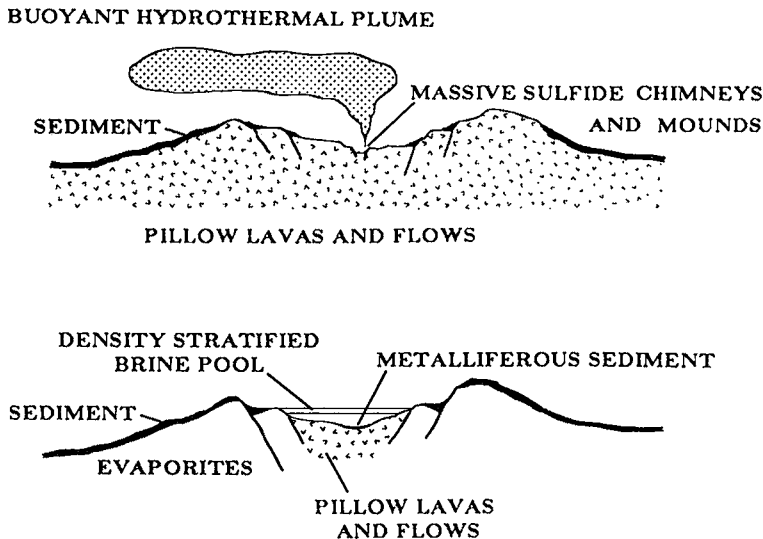

FIG. 2. Schematic diagram contrasting the depositional setting of ridge-crest hydrothermal deposits which form buoyant plumes, such as those found at 21°N EPR, with the deposition of metalliferous sediment beneath a brine pool, as exemplified by the Atlantis II Deep.
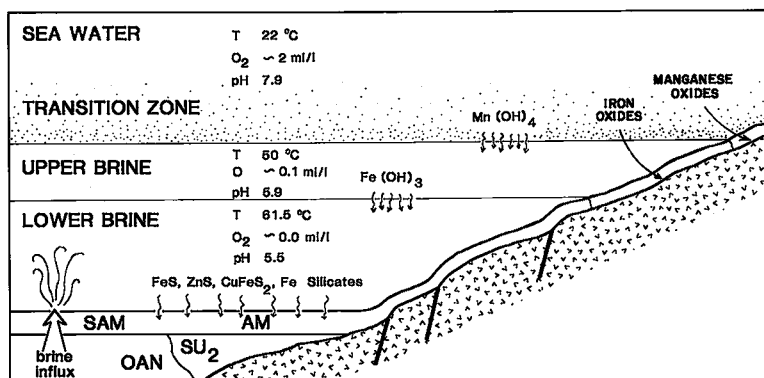
FIG. 3. Schematic representation of precipitation reactions within the density-stratified brine pool of the Atlantis II Deep. Diagram modified from Bischoff (1969) and Hartmann (1973).

mal fluid can be derived from the mineralogy of epigenetic features, including veins and replaced and recrystallized metalliferous sediment, which formed after deposition of metalliferous sediment in response to influx of hot brine through the metalliferous sediment. The veins are typically less than 1 cm wide and are filled with anhydrite or talc with subsidiary smectite and sulfide (Zierenberg & Shanks 1983, Pottorf & Barnes 1983, Oudin et al. 1984). The epigenetic veins are mineralogically similar to chimney deposits, but have formed within the unconsolidated sediments of the Deep instead of directly on the seafloor.

Chemical and mineralogical data together with phase equilibria show that higher temperature veins are dominated by talc and magnesian smectite, whereas lower temperature veins contain abundant anhydrite and ferroan smectite (Zierenberg & Shanks 1983). Isotopic study of epigenetic features was undertaken to evaluate the sources of metalliferous sediments, the importance of fluid mixing in the precipitation processes, and the range of temperatures involved.

SAMPLING AND ANALYTICAL METHODS

Most of the samples studied are subsamples of piston and kasten cores taken during the RV WANDO RIVER 1969 and VALDIVIA cruises of 1971 and 1973 (Fig. 1). Complete sample descriptions and a sample location map have been presented in Zierenberg & Shanks (1983). Samples 81 BC and 84 BC are boxcore samples of the uppermost metalliferous sediments collected during the 1979 INDOMED cruise of the RV MELVILLE. Samples from core 268K, taken in the Southwest Basin, are described by Oudin et al. (1984).

The isotopic data are presented in Tables A and B in the appendix. Samples are divided in two general groups. The group termed epigenetic precipitates (Table A) is predominantly vein material, but includes metalliferous sediment that recrystallized or was replaced at high temperature because of the flux of hot brine through the sediment or intrusion of basalt into unconsolidated mud (Zierenberg & Shanks 1983, Oudin et al. 1984). The group termed brine-pool precipitates (Table B) is characterized by very fine-grained, thinly laminated metalliferous sediments and is typical of the Atlantis II Deep sediment. Most of this material precipitated within the quiescent, anoxic lower brine, but some precipitated at interfaces between brines of differing salinities (Fig. 3). This material also contains minor amounts of pelagic sediment, material that recrystallized diagenetically from reaction with stagnant pore water (Weber-Diefenbach 1977), and resedimented metalliferous sediment derived from steep walls flanking the brine pool (Zierenberg & Shanks 1983).

Samples were washed with deionized water to remove interstitial salt. Anhydrite analyzed for sulfur, oxygen, and strontium isotopes was separated by hand-picking under a binocular microscope, with the exception of samples from talc veins where fine grain size prohibited physical separation of enough anhydrite both for oxygen and sulfur isotope determinations. Talc vein samples therefore were leached with cold deionized water to remove anhydrite sulfate for sulfur isotope analysis. Anhydrite separates were also dissolved in cold deionized water. The sulfate leachates were filtered to remove fine-grained included sulfides, and were reprecipitated as $BaSO_4$. Although gypsum occurs in some samples, textural evidence (Zierenberg & Shanks 1983) indicates it is not a primary precipitate, but forms by hydration of anhydrite during core storage. The hydration reaction does not produce any significant change in $\delta^{34}S$ values.

Sphalerite and pyrite, the predominant sulfides in most samples, were separated chemically because their fine grain size precluded physical separation. Samples were reacted at 60°C in 6N HCl while purging with N_2 gas. H_2S produced from sphalerite (along with minor amounts of pyrrhotite) was precipitated as Ag_2S. Residues from the sphalerite reaction, consisting predominantly of pyrite and silicates plus minor chalcopyrite, were leached with boiling aqua regia – bromine to oxidize pyrite and chalcopyrite to sulfate, which was precipitated as barium sulfate. Precipitated $BaSO_4$ was reduced with graphite under nitrogen and the resulting sulfide was precipitated as Ag_2S. Ag_2S was reacted with Cu_2O *in vacuo* to produce SO_2. Isotopic composition was standardized with McMaster Reference Standards (Rees 1978).

Oxygen isotope ratios of sulfate were determined on CO_2 obtained by reduction of $BaSO_4$ with graphite as described by Nehring *et al.* (1977). Oxygen isotope values of sulfate were normalized to a value of 9.6 for seawater sulfate (Zierenberg & Shanks 1986).

Hand-picked anhydrite was dissolved in HCl for strontium isotopic analysis. Bulk samples of talc veins and of a magnetite–hematite–pyroxene assemblage were completely digested in $HClO_3$–HF. Strontium contents of anhydrite samples were measured by atomic absorption spectroscopy. Strontium isotope ratios were measured on a multiple-collector mass spectrometer. Duplicate mass spectrometer runs had an average standard deviation (1σ) of 0.000056.

Oxygen was extracted from silicates and oxides by fluorination with BrF_5, and $\delta^{18}O$ data are reported relative to the SMOW standard. Magnetite, hematite and pyroxene were separated by isodynamic magnetic separation followed by hand-picking under a binocular microscope. Smectites analyzed for $\delta^{18}O$ are splits of samples previously analyzed by X-ray diffraction and electron microprobe (Zierenberg & Shanks 1983). Samples were treated with sodium citrate – dithionate to remove free iron oxide (Jackson 1979) and a $<2\mu m$ fraction was separated by centrifugation. X-ray diffraction indicated that the separates were monomineralic.

Manganoan siderite was reacted with anhydrous phosphoric acid at 50°C to produce CO_2 for carbon and oxygen isotope analysis. The acid fractionation factor used to correct the data for siderite reaction at 50°C was 1.01040 (Rosenbaum & Sheppard 1986). The $\delta^{18}O$ data are reported relative to Standard Mean Ocean Water (SMOW) assuming a CO_2 – H_2O fractionation of 1.0412 (Friedman & O'Neil 1977). The $\delta^{13}C$ data are calibrated to the Peedee Belemnite (PDB) standard.

RESULTS AND DISCUSSION

Sulfide $\delta^{34}S$ analyses (Fig. 4a) range from 2.5 to 23.4‰. However, the three high $\delta^{34}S$ values (14 – 23.4‰) are for very fine-grained pyrite inclusions in anhydrite which probably formed by reduction of a very small amount of anhydrite sulfate. This type of sulfide is volumetrically insignificant and is not typical of sulfides in the veins. If these anomalous samples are eliminated, the range of $\delta^{34}S$ values for vein sulfides is from 4.5 to 10.5‰, with a mean of 5.6 ± 1.4 (1σ). The average $\delta^{34}S$ value of vein sulfides coincides with values in both the presently forming sediments and the two older sulfide zones of the Atlantis II Deep, which have $\delta^{34}S$ values averaging 5.4‰ (range of ~1 to 15‰, Kaplan *et al.* 1969, Shanks & Bischoff 1980). The narrow range of $\delta^{34}S$ values for sulfides in epigenetic veins is consistent with precipitation from an incoming hydrothermal fluid in which all of the sulfur is present as H_2S and there is no isotopic exchange between oxidized and reduced sulfur species (Ohmoto 1972).

The determination of $\delta^{34}S$ values for coexisting sphalerite and pyrite in several samples allows calculation of equilibrium isotope-fractionation temperatures (Ohmoto & Rye 1979). The calculated values range from 50 to >800°C. Such anomalously high temperatures reflect incomplete separation of the phases during chemical dissolution or, more likely, isotopic disequilibrium during sulfide precipitation, as observed at 21°N EPR (Zierenberg *et al.* 1984).

Interaction of hydrothermal fluid with rift-zone basalts is indicated by isotopic studies of helium (Lupton *et al.* 1977), lead (Delevaux & Doe 1974), and strontium (Faure & Jones 1969, Zierenberg & Shanks 1986) in the Atlantis II brine, and from the inferred high temperatures for the ascending hydrothermal fluid (Shanks & Bischoff 1977, Pottorf & Barnes 1983). Leaching of basaltic sulfur by hydrothermal fluid has been demonstrated experimentally (Mottl *et al.* 1979). However, the $\delta^{34}S$ value of sulfide in the metalliferous sediment is approximately 5‰ higher than basaltic sulfide, requiring an additional source of isotopically heavy sulfur for the hydrothermal fluid.

The most likely source of the ^{34}S-enrichment is sulfate from seawater or evaporites. Reduction to sulfide presumably occurred in the hydrothermal fluid. The most abundant reducing agent is ferrous iron, present either in subsurface basalts or in ascending iron-rich fluid. Reduction of seawater sulfate has also been postulated to account for the similar range of $\delta^{34}S$ values (1.5 to 5.7‰) in sulfides from 21°N EPR and from the Juan de Fuca Ridge (Shanks & Seyfried 1987, Woodruff & Shanks 1988, Shanks *et al.* 1981, Styrt *et al.* 1981, Zierenberg *et al.* 1984), as well as in sulfides from ancient volcanogenic massive sulfide deposits.

Variations in the $\delta^{34}S$ value of sulfide minerals in the metalliferous sediment may reflect processes occurring within the brine pool or the sediment,

a)   ATLANTIS II DEEP SULFIDES

b)   ATLANTIS II DEEP SULFATES
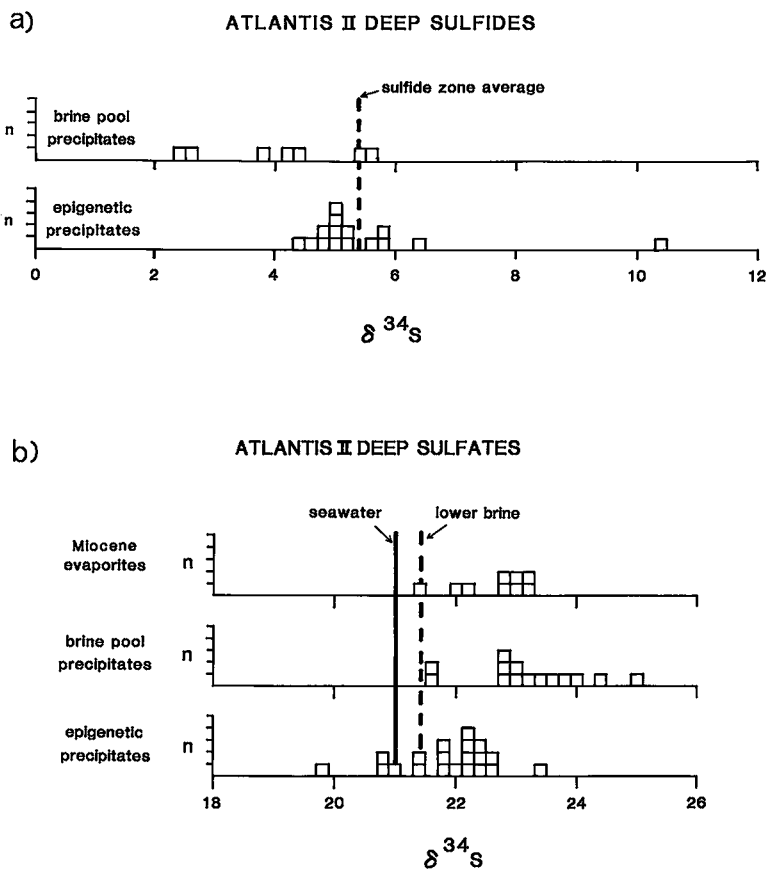

FIG. 4. (a) Distribution of $\delta^{34}S$ values from sulfide minerals from brine-pool precipitates and epigenetic precipitates. The arrow labeled "sulfide zone average" indicates the average of 29 samples from the upper and lower sulfide zones reported by Shanks & Bischoff (1980). (b) Distribution of $\delta^{34}S$ values of sulfates from epigenetic and brine-pool precipitates. Values for seawater, Atlantis II lower brine and DSDP 227 evaporites from Zierenberg & Shanks (1986).

rather than fluctuation of $\delta^{34}S$ in the incoming fluid. Although no biogenic reactions are known to occur at present in the Atlantis II Deep (Trüper 1969), very low $\delta^{34}S$ values in sulfide from some units of metalliferous sediment (–25 to –45‰) indicate bacterial reduction of sulfate during times when a hot brine pool was not present (Shanks & Bischoff 1980, Shanks 1983). Alternatively, organic-rich sediments containing biogenic sulfide from the fringes of the Deep could have been incorporated into the metalliferous sediments by tectonically induced resedimentation or by changes in the level of the brine pool.

Brine mixing and anhydrite precipitation

Veins in metalliferous sediment contain anhydrite coprecipitated with pyrrhotite, isocubanite, and iron-rich sphalerite, and could not have precipitated in chemical equilibrium (Pottorf & Barnes 1983). Sulfur in coexisting sulfide and sulfate is not in isotopic equilibrium. Pottorf & Barnes (1983) proposed fluid mixing of a hot, reduced hydrothermal fluid with a cooler, sulfate-bearing fluid to explain the observed mineral assemblages. Disequilibrium assemblages of anhydrite coprecipitated with pyrrhotite and isocubanite are characteristic of sulfide–sulfate chimneys formed at submarine hot springs (Goldfarb *et al.* 1983, Haymon 1983, Oudin 1983). Mixing of 350°C hydrothermal fluid, which is in equilibrium with pyrrhotite, with cold, sulfate-bearing seawater at the vent sites causes anhydrite and pyrrhotite to coprecipitate even though they are not in chemical or isotopic equilibrium (Janecky &

Seyfried 1984, Zierenberg & Shanks 1983). The sulfur, oxygen, and strontium isotopic ratios for the sulfate minerals in Atlantis II Deep metalliferous sediments also suggest that fluid mixing was an important process leading to the precipitation of metalliferous sediment.

Sulfate in the Atlantis II Deep hydrothermal system can be derived from two sources, seawater sulfate and sulfate dissolved from Miocene evaporites which flank the Deep (Zierenberg & Shanks 1986). Dissolved sulfate in the Atlantis II lower brine has a $\delta^{34}S$ value between that of seawater sulfate and sulfate in samples of Miocene evaporite recovered in DSDP hole 227, drilled 3 km east of the Atlantis II Deep (Fig. 4b). The $\delta^{34}S$ values for sulfate minerals from epigenetic precipitates range from the value of the lower brine (21.4‰) to about 2‰ higher. The $\delta^{34}S$ values for brine-pool sulfate precipitates are higher and are similar to those of the evaporites, with some samples even more enriched in ^{34}S than the evaporites (Fig. 4b).
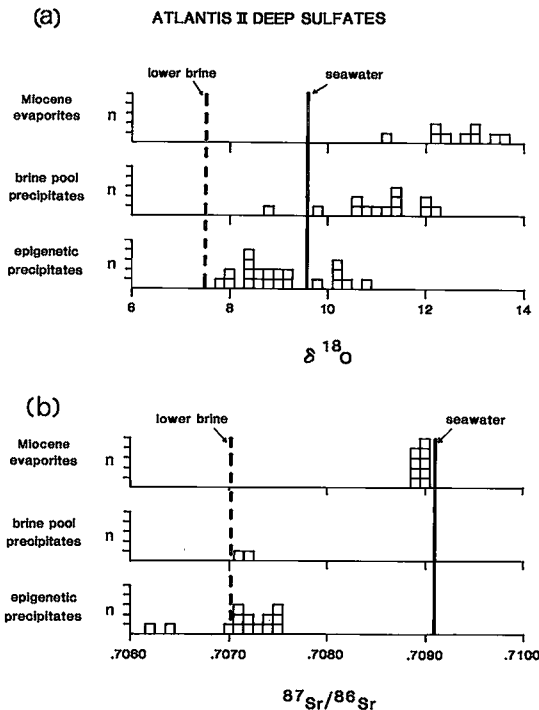

FIG. 5. (a) Distribution of $\delta^{18}O$ values of sulfates from epigenetic and brine-pool precipitates. Values for seawater, Atlantis II lower brine, and DSDP 227 evaporites from Zierenberg & Shanks (1986). (b) Distribution of $^{87}Sr/^{86}Sr$ ratios for anhydrite, talc-rich, and magnetite-hematite-rich samples from epigenetic and brine-pool precipitates. Values for seawater, Atlantis II lower brine and DSDP 227 evaporites from Zierenberg & Shanks (1986).

The $\delta^{34}S$ value of one epigenetic sulfate sample is significantly less than the $\delta^{34}S$ value of the lower brine (Fig. 4b). This sample is from a talc vein with very finely disseminated anhydrite that could not be separated by hand-picking. Sulfate from this sample was obtained by leaching with cold deionized water and probably includes sulfate derived from oxidation, during core storage, of isotopically lighter sulfide minerals.

The $\delta^{18}O$ values for sulfate minerals range from 7.8 to 12.2‰ (Fig. 5a). The $\delta^{18}O$ values of epigenetic sulfates range from those of the lower brine sulfate to about 3‰ higher; the range of $\delta^{18}O$ in brine-pool precipitates is significantly higher than in epigenetic veins, but not as high as in the evaporites.

The $\delta^{34}S$ and the $\delta^{18}O$ values in sulfate of the metalliferous sediment could be interpreted as derived from a two-component mixture of an isotopically lighter "hydrothermal" component similar to the lower brine sulfate, and an isotopically heavier end member similar to the sulfate in Miocene evaporites. Definition of the mixing process is complicated by isotopic fractionation and exchange. The epigenetic sulfates seem to contain a significant "hydrothermal" component, whereas some of the brine-pool precipitates are similar to the "evaporitic" component.

Unfortunately, such an interpretation cannot fully explain the data. The $\delta^{34}S$ values of evaporites recovered from DSDP 227 are too low to account for the ^{34}S-enrichment found in some of the brine-pool precipitates. This difference could be a sampling bias because only the upper 130 m of the evaporites were penetrated by Hole 227, whereas the evaporite sequence is 2–4 km thick (Stoffers & Kühn 1974). A more substantial argument against conservative mixing of two sulfate sources is that it should result in a linear correlation between $\delta^{34}S$ and $\delta^{18}O$. Instead, the isotope values show almost no correlation ($r^2 = 0.18$).

A second explanation of the overall variation in sulfate $\delta^{18}O$ data involves temperature-dependent fractionation. Although there is no significant oxygen isotope fractionation between dissolved sulfate and anhydrite (Chiba et al. 1981), dissolved sulfate can exchange oxygen isotopes with the H_2O in the hydrothermal fluid prior to precipitation. The low-$\delta^{18}O$ value of dissolved sulfate in the lower brine may be a reflection of the high-temperature history of the brine. A temperature of 225°C can be calculated by assuming equilibrium fractionation of $\delta^{18}O$ between H_2O in the brine (1.21‰, Craig 1969, Schoell & Faber 1978) and dissolved lower brine sulfate. Similar calculations for the epigenetic precipitates indicate temperatures of 200 to 260°C, and for the brine-pool precipitates, 180 to 235°C. Fluid inclusions in one sample of vein anhydrite gave an average pressure-corrected filling temperature of

238°C (Pottorf & Barnes 1983). Oudin *et al.* (1984) reported fluid-inclusion filling temperatures of 250 to 420°C in epigenetic anhydrite. The highest temperatures cannot represent trapping temperatures of a homogeneous fluid because they are in excess of the *in situ* boiling temperature of the lower brine. An *in situ* boiling temperature of $\approx 390°C$ is calculated by assuming 4.4 molal NaCl equivalency for the lower brine using the $NaCl–H_2O$ data of Phillips *et al.* (1981). Although the oxygen isotope data appear to reflect temperature-dependent fractionation, the calculated high temperatures and the poor correlation with smectite oxygen isotope temperatures (see below) suggest that sulfate does not maintain oxygen isotope equilibrium during precipitation of anhydrite at lower temperatures. Instead it appears that sulfate oxygen isotope values are "quenched", thereby preserving a record of the high-temperature history of the hydrothermal fluid. Preservation of sulfate oxygen isotope values obtained at high temperature is consistent with the sluggish kinetics of sulfate isotopic exchange at temperatures $<200°C$ (Ohmoto & Lasaga 1983).

The $^{87}Sr/^{86}Sr$ ratios of 10 hand-picked anhydrite samples and three bulk digestions of talc-vein samples having complex mineralogy show a narrow range of $^{87}Sr/^{86}Sr$ values from 0.7070 to 0.7075 (Fig. 5b). The $^{87}Sr/^{86}Sr$ ratios of the epigenetic and brine-pool precipitates are close to those of the Atlantis II lower brine, but allow for a minor admixture of strontium from seawater or evaporites. The strontium isotope ratio of the lower brine indicates that some of the dissolved strontium is derived from basalt during water–rock interaction (Faure & Jones 1969, Zierenberg & Shanks 1986). Contribution of strontium to the epigenetic precipitates from a fluid which has interacted only with the Miocene evaporites is limited to a small amount by isotope and mass balance constraints, because strontium concentrations in the Miocene evaporites (14–5000 ppm, Stoffers & Kühn 1974, Zierenberg & Shanks 1986) exceed the concentration in the lower brine (46 ppm, Zierenberg & Shanks 1986).

In summary, mineral assemblages of the epigenetic precipitates indicate mixing of a high-temperature, reduced fluid with a sulfate-bearing fluid. Variations in sulfur, oxygen and strontium isotopic ratios between epigenetic and brine-pool precipitates suggest that the sulfate-bearing fluid has variable isotopic composition due to contributions from multiple sources. Major temporal variations in brine composition seem plausible when one considers the large influx of brine necessary to precipitate the >15-m thickness of metalliferous sediment. For example, if all the dissolved Si, Fe, Zn, and Cu in the lower brine were precipitated, the uncompacted metalliferous sediment would form a layer less than 9 cm thick. Therefore, many times the present volume of

brine must have circulated through the system to account for the observed thickness of metalliferous sediment. In fact, the laminated nature of the metalliferous sediment reflects variable chemical and (or) physical conditions in the brine pool that probably relate to variable influx and composition of hydrothermal brine.

Sulfate in the present-day brine pool is isotopically more similar to the epigenetic vein minerals than sulfates that have precipitated in the brine pool in the recent past ($<10,000$ years, Shanks & Bischoff 1980). Epigenetic features are most common in the Southwest Basin of the Atlantis II Deep (Zierenberg & Shanks 1983), which is the site of active hydrothermal venting (Schoell 1976). It thus appears that the epigenetic features are related to the most recent phase of hydrothermal venting.

Origin of carbonate minerals

Fe–Mn carbonate in metalliferous sediment forms by precipitation from hydrothermal brine and by replacement of detrital biogenic carbonate. It is a minor constituent in anhydrite and sulfide beds, where it occurs as aggregates of euhedral rhombohedra, and locally forms individual beds (Bischoff 1969, Bäcker 1976). Optical petrography and scanning electron microscopy revealed that some aggregates of rhombohedral crystals replaced and overgrew planktonic microfossils. Energy-dispersion X-ray spectroscopy on the scanning electron microscope, and X-ray diffraction indicate that the carbonates range from siderite to rhodochrosite and contain minor amounts of Ca and Mg. Carbonates have not been observed within epigenetic veins; isotope values in Table A in the appendix are for carbonates from metalliferous sediment of vein walls.

Seven analyzed Fe–Mg carbonate samples have $\delta^{13}C$ values ranging from –3.9 to 1.6‰ (PDB scale) and $\delta^{18}O$ values ranging from 21.4 to 32.3‰ (SMOW scale). Oxygen isotope temperatures were calculated assuming equilibrium with water of the same isotopic composition as the present lower brine ($\delta^{18}O = 1.21$‰, Craig 1969, Schoell & Faber 1978), and using the fractionation equation for siderite-water ($10^3 \ln \alpha = 2.89 \ 10^6 T^{-2}–2.76$, calculated from the data of Becker & Clayton 1976). A potential problem is the application of the siderite–water equation to a Mn–Fe carbonate phase. The fractionation curve for rhodochrosite–water has not been determined, but a single measurement at 240°C by O'Neil *et al.* (1969) suggests slightly less fractionation between rhodochrosite and water than between siderite and water. Therefore, application of the siderite–water fractionation equation to rhodochrosite results in calculated oxygen isotope temperatures that are too high (approximately 8% difference at 240°C).

Oxygen isotope temperatures calculated from the siderite–water fractionation equation range between 47 and 61°C, except for the two extreme values of 19 and 82°C. The calculated temperatures are similar to temperatures measured in the lower brine since 1965 (54 to 62°C).

There are two sources for the carbonate minerals: biogenic debris precipitated from Red Sea water carbonate ($\delta^{13}C$ = -1.5‰, Schoell & Stall 1972) and carbonate dissolved in the lower brine ($\delta^{13}C$ = -7‰, Schoell & Stall 1972). We have calculated $\delta^{18}O$ and $\delta^{13}C$ values of carbonate that should ideally precipitate from normal Red Sea Deep water and from the Atlantis II lower brine. Oxygen isotope values were calculated from the siderite–water equation using the ambient T and $\delta^{18}O$ characteristics of Red Sea water (22°C, $\delta^{18}O$ = 1.89‰, Schoell & Faber 1978) and of the lower brine ($\delta^{18}O$ = 1.21‰, Craig 1969, Schoell & Faber 1978; 110°C, which is the highest temperature measured for smectite precipitated from the brine pool). Carbon isotope values were calculated from the calcite–HCO_3^- fractionation ($10^3 \ln \alpha$ = 0.095 $10^6 T^{-2}$ -2.76; Deines *et al.* 1974), assuming this applies to siderite–HCO_3^-. A plot of $\delta^{13}C$ *versus* $\delta^{18}O$ for the calculated carbonate end-members and the brine-pool precipitates (Fig. 6) indicates that isotopic data are generally consistent with the two sources of carbon indicated by petrographic observations.
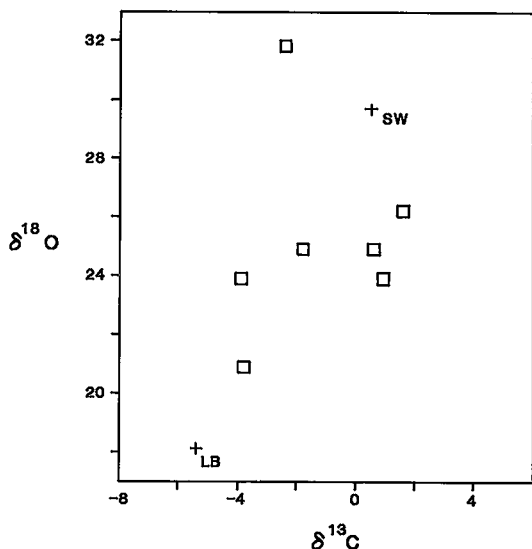

FIG. 6. $\delta^{13}C$ *versus* $\delta^{18}O$ for Fe–Mn carbonate from the metalliferous sediment. The Fe–Mn carbonate is a mixture of replaced biogenic carbonate and inorganic carbonate precipitated from hydrothermal fluids. Points SW and LB are calculated compositions, respectively, of siderite in equilibrium with Red Sea water (22°C, $\delta^{18}O$ = 1.89, $\delta^{13}C$ = 1.5) and Atlantis II lower brine (110°C, $\delta^{18}O$ = 1.21, $\delta^{13}C$ = -7.0).

The magnetite–hematite–pyroxene zone

The magnetite–hematite–pyroxene assemblage, which occurs in a limited area in the northern part of the Southwest Basin (Fig. 1), formed by the high-temperature recrystallization of fine-grained goethitic and hematitic sediment (Zierenberg & Shanks 1983). Recrystallization apparently is related to a local temperature anomaly caused either by venting of high-temperature hydrothermal fluid, or by localized convection of pore fluids driven by heat from the intrusion of basalt into the metalliferous mud. Mass-balance calculations show that the transformation of hematite to magnetite requires large amounts of reducing agent, probably ferrous iron, and thus precludes isochemical recrystallization in response to a local temperature anomaly (Zierenberg & Shanks 1983). A high flux of reduced hydrothermal fluid through the sediment is required for the transformation.

The $^{87}Sr/^{86}Sr$ ratio of one bulk sample of the magnetite–hematite–pyroxene assemblage (0.70718) is similar to the value of the lower brine and falls in the range for the epigenetic anhydrite and talc samples. Two of the magnetite-rich samples have slightly lower values (0.70616, 0.70635), possibly reflecting the presence of the minor amounts of basaltic debris in these samples with an $^{87}Sr/^{86}Sr$ ratio of ≈0.7027 (Cohen *et al.* 1980).

Oxygen isotope ratios were determined for five separates of magnetite, one of hematite, and two of pyroxene. Four magnetite samples from cores 17P and 18P have a narrow range of $\delta^{18}O$, from -3.2 to -3.5‰, whereas a magnetite sample from core 492K has a $\delta^{18}O$ value of -5.1‰. Hematite coexisting with magnetite from core 492 K is enriched in $\delta^{18}O$ by 0.4‰; because of the higher oxidation state of hematite this result would be expected if the pair formed in isotopic equilibrium (O'Neil 1977).

The two samples of pyroxenes from cores 18P and 492K have $\delta^{18}O$ values of 0.9 and 1.2‰, respectively. Application of the magnetite–pyroxene fractionation equation (Matthews *et al.* 1983) yields temperatures of 718°C and 526°C, much too high to be reasonable equilibrium temperatures. An upper temperature limit is set by the *in situ* boiling point of the lower brine (≈390°C).

The oxygen isotope fractionation betwen pyroxene and water can be estimated by linear extrapolation to lower temperature of the data in Table 8 of Matthews *et al.* (1983). Fractionation is given by the equation 1000 in α (*Px*–H_2O) = $10^6 T^{-2}$ - 2.92. If it is assumed that the pyroxene formed in equilibrium with water of the same isotopic composition as the present brine (1.21‰), then the calculated temperature of formation of the two samples is 346°C (core 18P) and 313°C (core 492K). These temperatures are consistent with the observed mineral assemblage (Zierenberg & Shanks 1983). The magnetite–

hematite–pyroxene zone was probably formed by localized brine convection caused by surplus heat, such as might be provided by a basaltic sill. The presence of basaltic debris at the base of cores 492K and 17P is consistent with this hypothesis. Influx of high-temperature hydrothermal fluid could also provide the heat and reductant necessary for the transformation of hematite to magnetite. However, the magnetite–hematite–pyroxene is a low-sulfur assemblage containing only minor chalcopyrite and lacking pyrrhotite or pyrite, and is therefore not consistent with the mineral assemblage that typically precipitates from the incoming hydrothermal fluid.

Smectite geothermometry

Oxygen isotope ratios were determined for 16 smectite samples and one chlorite sample. Temperatures, calculated using the smectite–water fractionation equation of Yeh & Savin (1977) and the measured $\delta^{18}O$ value of H_2O in the lower brine, range from 62 to 110°C for brine-pool precipitates, and from 146 to 271°C for epigenetic precipitates. A temperature of 250°C is obtained for the chlorite sample using the chlorite–H_2O fractionation equation (Wenner & Taylor 1971).
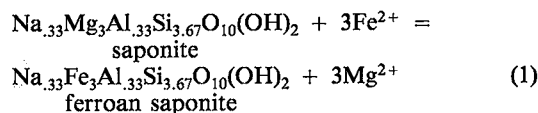
Cole (1983) computed oxygen isotope temperatures for smectite from three cores from the Southwest Basin of the Atlantis II Deep. Cole classified the clay minerals as either nontronite or montmorillonite/beidellite based on X-ray diffraction patterns (Cole 1983, Cole & Shaw 1983). The oxygen isotope temperatures for nontronite range from 78 to 139°C, and for montmorillonite/beidellite from 162 to 206°C. Chemical analyses of the clay with montmorillonite/beidellite XRD characteristics showed that the mineral is an iron-rich smectite (Cole 1988).

Zierenberg & Shanks (1983) classified smectite from the Atlantis II Deep as belonging to the saponite – ferroan saponite – nontronite series on the basis of both XRD characteristics and chemical data. Nontronite was interpreted to have precipitated in the brine pool. Epigenetically precipitated smectite is predominantly trioctahedral and ranges in composition from ferroan saponite to saponite. Badaut *et al.* (1985) have shown that both dioctahedral nontronite and trioctahedral ferroan saponite occur in Atlantis II Deep metalliferous sediment. Nontronite was recovered from the North Basin, an area distant from active hydrothermal vents. Ferrous iron in saponite recovered from the area of active venting in the Southwest Basin is rapidly oxidized under normal laboratory conditions (Badaut *et al.* 1985).

On the basis of geochemical calculations using thermodynamic data estimated for end-member clay minerals, Zierenberg & Shanks (1983) suggested that magnesium-rich smectite in the Atlantis II Deep formed at higher temperature than iron-rich varie-

ties. This hypothesis can be tested using the oxygen isotope temperatures calculated for Atlantis II Deep smectite.

The exchange reaction between saponite and ferroan saponite can be written as:

$$Na_{.33}Mg_3Al_{.33}Si_{3.67}O_{10}(OH)_2 \ + \ 3Fe^{2+} \ =$$
$$\text{saponite}$$
$$Na_{.33}Fe_3Al_{.33}Si_{3.67}O_{10}(OH)_2 \ + \ 3Mg^{2+} \qquad (1)$$
$$\text{ferroan saponite}$$

The mass-action expression for equation (1) is:

$$K \ = \ \frac{a_{\text{FE-SAP}} \ (a_{Mg})^3}{a_{\text{SAP}} \ \ (a_{Fe})^3} \qquad (2)$$

The equilibrium constant is proportional to the activity ratio of the ions in solution (a_{Fe}, a_{Mg}) and the activity ratio of the smectite end-members in the solid solution ($a_{\text{FE-SAP}}$, a_{SAP}). Some simplifying assumptions facilitate the qualitative interpretation of the trend of the chemical and isotopic data for the smectites. If solid solution in smectite is ideal, or if the activity coefficients for the two end members are nearly constant, then the equilibrium constant will be directly proportional to the respective mole fractions in the smectite solid solution, for a fixed iron-to-magnesium activity ratio in the fluid. Changes in the equilibrium constant with temperature are given by:

$$\frac{\ln K}{(1/T)} \ = \ \frac{-\Delta H_r^\circ}{R} \qquad (3)$$

If H_r° is relatively constant over the temperature interval of interest, ln (Fe/Mg) (atomic) of the smectite should show an approximately linear variation with $(1/T)$. Values of ln (Fe/Mg) in the octahedral layer of the smectite have been calculated from the chemical data of Zierenberg & Shanks (1983). A plot of these values against oxygen isotope temperatures shows a strong linear correlation ($r^2 = 0.91$, Fig. 7). Data presented in Cole (1988) show a similar relationship.

Some precautionary comments are in order regarding this geothermometer, especially as applied to the Atlantis II Deep. The fractionation equation for smectite–water (Yeh & Savin 1977) is estimated from data on natural montmorillonite and comparison to the illite–water system, and therefore is not precisely calibrated. Also, isotopic fractionation in smectite might be a function of composition as well as of temperature. However, octahedral substitution in other Fe–Mg silicates does not significantly affect oxygen isotope fractionation (Matthews *et al.* 1983).

The range of $\delta^{18}O$ in the smectites could also result from the mixing of isotopically distinct waters. However, if the smectite formed at constant temper-
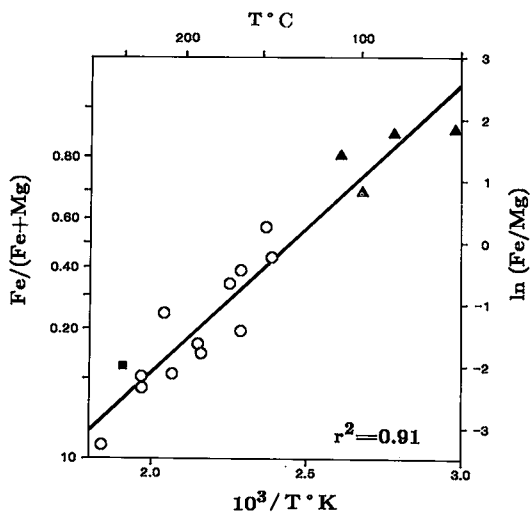
Fig. 7. Plot of $10^3/T$ K calculated from the smectite-water oxygen isotope fractionation equation of Yeh & Savin (1977) *versus* ln (Fe/Mg) (atomic) ratio for the octahedral sites of smectite from brine-pool precipitates (triangles) and epigenetic precipitates (circles). A single chlorite sample (square) is shown for comparison, but was not used to calculate the least-squares regression line ($r^2 = 0.91$).

ature, end-member solutions must have differed in $\delta^{18}O$ by at least 15‰, which is not considered reasonable as there are no local water sources with such differences in isotope composition. The existence of waters having large variations in $\delta^{18}O$ also is not consistent with the isotopic ratios of sulfates coexisting with smectite, and it does not account for the correlation of oxygen isotope temperatures with smectite compositions.

A more important constraint on the use of the smectite geothermometer is evident from inspection of equation (2). The equilibrium constant is also a function of the activity ratios of ionic iron and magnesium in solution. The assumption of a constant activity ratio of these ions is probably not justifiable. Mixing of solutions of different compositions will change the iron-magnesium ratio in the smectite, and this change will not be a strict function of temperature. However, in order to account for the correlation (Fig. 7) by mixing alone, the incoming hydrothermal fluid would have to have been both hotter and to have a higher activity ratio of magnesium to iron than the brine-pool fluid with which it mixed. This is unlikely given that basalt–seawater experiments (Bischoff & Dickson 1975, Seyfried & Bischoff 1977, Mottl *et al.* 1979) and studies of the hydrothermal system at 21°N, EPR (Von Damm *et al.* 1985) indicate that reaction of a seawater-like fluid with hot basalt leads to magnesium depletion

and iron enrichment in the fluid. Therefore, if fluid mixing was the only process controlling smectite chemistry we might expect that the high-temperature fluid would form Fe-rich smectite, contrary to the observations.

Even if the concentrations of magnesium and iron in solution remain constant, the activity ratio of the ions will not be constant because of temperature changes which will affect the activity coefficients. It is not possible to separate the effects of the temperature dependence of the equilibrium constant from the effects of changes in the activities of the ions in solution because we lack detailed knowledge both of the chemical composition of the incoming hydrothermal fluid and chemical speciation models valid for saline solutions at high temperature.

Calculation of the equilibrium constant for reaction (1) using estimated thermodynamic data for smectite end-members (Zierenberg & Shanks 1983) and the SUPCRT computer code (Helgeson *et al.* 1978) indicates that the equilibrium constant changes by about two orders of magnitude over the temperature interval calculated from the smectite oxygen-isotope composition (Table 1). Mg-Fe exchange in smectite is thus typical of most silicates in that the smaller Mg^{2+} ion is favored at higher temperature.

TABLE 1. EQUILIBRIUM CONSTANT FOR THE REACTION OF SAPONITE TO FERROAN SAPONITE AT 200 BARS.

Temperature	60°C	100°C	150°C	200°C	250°C	300°C
Log K	13.2	12.5	11.8	11.4	11.1	10.8

The temperature range indicated by the smectite geothermometer is consistent with other estimates of the thermal history of the hydrothermal fluid. Brine-pool smectite was precipitated at temperatures of 62 to 110°C; the temperature of the lower brine is 62.3°C (Hartmann 1985, Monin & Plakhin 1982). Epigenetic smectite formed at temperatures of 146 to 271°C. This is within the temperature range of the incoming hydrothermal fluid, as estimated from silica and Na–Ca–K geothermometry, $\delta^{18}O$ data on sulfates, and the recent thermal evolution of the brine (Shanks & Bischoff 1977). In particular, the smectite geothermometry supports the interpretation of Pottorf & Barnes (1983) that most of the sulfide deposition occurs between 200 and 250°C, based on sulfide assemblages from veins and metalliferous sediment.

Authigenic smectite is a constituent of many active hydrothermal systems, and potentially can be used as a quantitative geothermometer. Variations in the Fe/(Fe + Mg) ratio of chemically precipitated metalliferous sediment potentially can be used to guide the explorationist to the higher temperature parts of ancient hydrothermal systems, and possibly to mineral concentrations that are not exposed at the

surface. Mg-rich smectite is the preferred high-temperature phase, especially in exhalative systems where hydrothermal fluid can mix with Mg-rich seawater.

High-temperature ($>200°C$) hydrothermal fluids associated with volcanogenic sulfide deposits may be devoid of Mg (Bischoff & Dickson 1975, Seyfried & Bischoff 1977, 1981, Von Damm et al. 1985). Recent studies of ancient volcanogenic deposits (Roberts & Reardon 1978, Richards & Cann 1988, Zierenberg et al. 1987) have shown that Fe-rich chlorite dominates the interiors of alteration zones, with Mg-rich phases in peripheral zones. In some cases, pervasive magnesium metasomatism occurs in altered rocks underlying massive sulfide deposits such as Mattagami Lake, Quebec (Costa et al. 1983) and Arctic (Schmidt 1988). This apparent contradiction is a result of the Mg-depleted nature of the ascending ore fluids due to water–rock interaction deeper in the system. The results of this study on the chemical and isotopic composition of Atlantis II Deep smectite indicate that Mg-rich phases are preferred in the upper or peripheral portions of the hydrothermal system where Mg-rich ambient seawater mixes with high-temperature ore-transporting fluid.

REFERENCES

BADAUT, D., BESSON, G., DECARREAU, A. & RAUTUREAU, R. (1985): Occurrence of a ferrous, trioctahedral smectite in Recent sediments of Atlantis II Deep, Red Sea. *Clay Minerals* 20, 389-404.

BÄCKER, H. (1976): Facies und chemische Zusammensetzung rezenter Ausfällungen aus Mineralquellen in Roten Meer. *Geol. Jahrb.* 17, 151-172.

_____ & RICHTER, H. (1973): Die rezente hydrothermal sedimentäre Lagerstätte Atlantis II-Tief in Roten Meer. *Geol. Rundsch.* 62, 697-740.

BECKER, R.H. & CLAYTON, R.N. (1976): Oxygen isotope study of a Precambrian banded iron-formation,

Hamersley Range, Western Australia. *Geochim. Cosmochim. Acta* 40, 1153-1165.

BIGNELL, R., CRONAN, D. & TOOMS, J. (1976): Metal dispersion in the Red Sea as an aid to marine geochemical exploration. *Inst. Mining Metall. Trans.* 84, B274-B278.

BISCHOFF, J.L. (1969): Red Sea geothermal brine deposits: Their mineralogy, chemistry and genesis. *In* Hot Brines and Recent Heavy Metal Deposits in the Red Sea (E.T. Degens & D.A. Ross, eds.), 368-401. Springer-Verlag, New York.

_____ & DICKSON, F.W. (1975): Seawater–basalt interaction at 200°C and 500 bars: Implications for origin of sea-floor heavy-metal deposits and the regulation of seawater chemistry. *Earth Planet. Sci. Lett.* 25, 385-397.

CHIBA, H., KUSAKABE, M., HIRAN, S. & SOMIYA, S. (1981): Oxygen isotope fractionation factors between anhydrite and water from 100 to 550°C. *Earth Planet. Sci. Lett.* 53, 55-62.

COHEN, R.S., EVENSEN, N.M., HAMILTON, P.J. & O'NIONS, R.K. (1980): U–Pb, Sm–Nd and Rb–Sr systematics of mid-ocean ridge basalt glasses. *Nature* 283, 149-153.

COLE, T.G. (1983): Oxygen isotope geothermometry and origin of smectites in the Atlantis II Deep, Red Sea. *Earth Planet. Sci. Lett.* 66, 166-176.

_____ (1988): The nature and origin of smectite in the Atlantis II Deep, Red Sea. *Can. Mineral.* 26, 755-763.

_____ & SHAW, H.F. (1983): The nature and origin of authigenic smectites in some recent marine sediments. *Clay Minerals* 18, 239-252.

COSTA, U.R., BARNETT, R.L. & KERRICH, R. (1983): The Mattagami Lake Mine Archean Zn–Cu sulfide deposit, Quebec: Hydrothermal coprecipitation of talc and sulfides in a sea-floor brine pool – Evidence from geochemistry, $^{18}O/^{16}O$, and mineral chemistry. *Econ. Geol.* 78, 1144-1203.

CRAIG, H. (1969): Geochemistry and origin of the Red Sea brines. *In* Hot Brines and Recent Heavy Metal Deposits in the Red Sea (E.T. Degens & D.A. Ross, eds.), 208-242. Springer-Verlag, New York.

DEGENS, E.T. & ROSS, D.A. (eds.) (1969): *Hot Brines and Recent Heavy Metal Deposits in the Red Sea.* Springer-Verlag, New York.

DEINES, P., LANGMUIR, D. & HARMON, R.S. (1974): Stable carbon isotope ratios and the existence of a gas phase in the evolution of carbonate ground waters. *Geochim. Cosmochim. Acta* 38, 1147-1164.

DELEVAUX, M.H. & DOE, B.R. (1974): Preliminary report on uranium, thorium and lead contents and

lead isotopic composition in sediment samples from the Red Sea. *Initial Reports Deep Sea Drilling Project* **23**, 943-946. U.S. Gov. Printing Office, Washington, D.C.

FAURE, G. & JONES, L.M. (1969): Anomalous strontium in the Red Sea brines. *In* Hot Brines and Recent Heavy Metal Deposits in the Red Sea (E.T. Degens & D.A. Ross, eds.), 243-250. Springer-Verlag, New York.

FRIEDMAN, I. & O'NEIL, J.R. (1977): Compilation of stable isotope fractionation factors of geochemical interest. *In* Data of Geochemistry, 6th Ed. (I. Freidman & J.R. O'Neil, eds.). *U.S. Geol. Surv. Prof. Pap.* **440-KK**.

GOLDFARB, M.S., CONVERSE, D.R., HOLLAND, H.D. & EDMOND, J.M. (1983): The genesis of hot spring deposits on the East Pacific Rise, 21°N. *Econ. Geol. Monogr.* **5**, 184-197.

HARTMANN, M. (1973): Untersuchung von suspendiertem Material in den Hydrothermallaugen des Atlantis II-Tiefs. *Geol. Rundsch.* **62**, 742-754.

_____ (1985): Atlantis II Deep geothermal brine system. Chemical processes between hydrothermal brines and Red Sea Deep water. *Geology* **64**, 157-177.

HAYMON, R.M. (1983): Growth history of hydrothermal black smoker chimneys. *Nature* **301**, 695-698.

_____ & KASTNER, M. (1981): Hot springs deposits on the East Pacific Rise at 21°N: preliminary description of mineralogy and genesis. *Earth Planet. Sci. Lett.* **53**, 363-381.

HELGESON, H.C. DELANY, J.M., NESBITT, H.W. & BIRD, D.K. (1978): Summary and critique of the thermodynamic properties of rock-forming minerals. *Amer. J. Sci.* **274**, 1199-1261.

JACKSON, M.L. (1979): *Soil Chemical Analysis – Advanced Course.* 2nd ed. 11th printing. Published by author, Madison, Wisconsin 53705.

JANECKY, D.R. & SEYFRIED, W.E., JR. (1984): Formation of massive sulfide deposits on the oceanic ridge crests: Incremental reaction models for mixing between hydrothermal solutions and seawater. *Geochim. Cosmochim. Acta* **48**, 2723-2738.

KAPLAN, I.R., SWEENEY, R.E. & NISSENBAUM, A. (1969): Sulfur isotope studies on Red Sea geothermal brines and sediments. *In* Hot Brines and Recent Heavy Metal Deposits in the Red Sea (E.T. Degens & D.A. Ross, eds.), 474-498. Springer-Verlag, New York.

KOSKI, R.A., CLAGUE, D.A. & OUDIN, E. (1984): Mineralogy and chemistry of massive sulfide deposits from the Juan de Fuca Ridge. *Geol. Soc. Amer. Bull.* **95**, 930-945.

LUPTON, J.E., WEISS, R.F. & CRAIG, H. (1977): Mantle helium in the Red Sea brines. *Nature* **266**, 244-246.

MATTHEWS, A., GOLDSMITH, J.R. & CLAYTON, R.N. (1983): Oxygen isotope fractionations involving pyroxenes: The calibration of mineral-pair geothermometers. *Geochim. Cosmochim. Acta* **47**, 631-644.

McDOUGALL, T.J. (1984a): Fluid dynamic implications for massive sulfide deposits of hot saline fluid flowing into a submarine depression from below. *Deep-Sea Research* **31**, 145-170.

_____ (1984b): Convective processes caused by a dense, hot saline source flowing into a submarine depression from above. *Deep-Sea Research* **31**, 1287-1309.

MOTTL, M.J., HOLLAND, H.D. & CORR, R.F. (1979): Chemical exchange during hydrothermal alteration of basalt by seawater – II. Experimental results for Fe, Mn, and sulfur species. *Geochim. Cosmochim. Acta* **43**, 869-884.

MONIN, A.S., LITVIN, V.M., PODRAZHANSKY, A.M., SAGALEVICH, A.M., SOROKHTIN, O.G., VOITOV, V.I., YASTREBOV, V.S. & ZONENSHAIN, L.P. (1982): Red Sea submersible research expedition. *Deep-Sea Research* **29**, 361-373.

_____ & PLAKHIN, E.A. (1982): Stratification and space-time variability of Red Sea hot brines. *Deep-Sea Research* **29**, 1271-1291.

_____, _____, PODRAZHANSKY, A.M., SAGALEVICH, A.M. & SOROKHTIN, O.G. (1981): Visual observations of Red Sea hot brines. *Nature* **291**, 222-225.

NAWAB, Z.A. (1984): Red Sea mining: a new era. *Deep-Sea Research* **31**, 813-822.

NEHRING, N.L., BROWN, P.A. & TRUESDELL, A.H. (1977): Techniques for the conversion to carbon dioxide of oxygen from dissolved sulfate in thermal waters. *Geothermics* **5**, 63-66.

OHMOTO, H. (1972): Systematics of sulfur and carbon isotopes in hydrothermal ore deposits. *Econ. Geol.* **67**, 551-578.

_____ & LASAGA, A.C. (1983): Kinetics of reactions between aqueous sulfates and sulfides in hydrothermal systems. *Geochim. Cosmochim. Acta* **46**, 1727-1746.

_____ & RYE, R.O. (1979): Isotopes of sulfur and carbon. *In* Geochemistry of Hydrothermal Ore Deposits (H.L. Barnes, ed.). 2nd ed., 509-567. Wiley-Interscience, New York.

O'NEIL, J.R. (1977): Stable isotopes in mineralogy. *Phys. Chem. Minerals* **2**, 105-123.

_____, CLAYTON, R.K. & MAYEDA, T.K. (1969): Oxygen isotope fractionation in divalent metal car-

bonates. *J. Chem. Phys.* **51**, 5547-5558.

OUDIN, E. (1983): Hydrothermal sulfide deposits of the East Pacific Rise (21°N) part I: Descriptive mineralogy. *Marine Mining* **4**, 39-72.

———, THISSE, Y. & RAMBOZ, C. (1984): Fluid inclusion and mineralogical evidence for high-temperature saline hydrothermal circulation in the Red Sea metalliferous sediments: Preliminary results. *Marine Mining* **5**, 3-31.

PHILLIPS, S.L., IGBENE, A., FAIR, J.A., OZBEK, H. & TAVANA, M. (1981): *A Technical Databook for Geothermal Energy Utilization.* L.B.L.-12810, Lawrence Berkeley Laboratories, Berkeley, California, 46p.

POTTORF, R. & BARNES, H.L. (1983): Mineralogy, geochemistry, and ore genesis of hydrothermal sediments from the Atlantis II Deep, Red Sea. *Econ. Geol. Monogr.* **5**, 198-223.

RICHARDS, H.G. & CANN, J.R. (1988): Mineralogical and metasomatic zonation of alteration pipes of Cyprus sulfide deposits. *Econ. Geol.* **83**, (in press).

REES, C.E. (1978): Sulphur isotope measurements using SO_2 and SF_6. *Geochim. Cosmochim. Acta* **42**, 383-389.

ROBERTS, R.G. & REARDON, E.J. (1978): Alteration and ore-forming processes at Mattagami Lake, Quebec. *Can. J. Earth Sci.* **15**, 1-21.

ROESER, H.A. (1975): A detailed magnetic survey of the southern Red Sea. *Geol. Jahrb.* **13**, 131-153.

ROSENBAUM, J. & SHEPPARD, S.M.F. (1986): An isotopic study of siderites, dolomites and ankerites at high temperatures. *Geochim. Cosmochim. Acta* **50**, 1147-1150.

SATO, T. (1972): Behaviours of ore-forming solutions in seawater. *Mining Geology* **22**, 31-42.

SCHMIDT, J.M. (1988): Mineral and whole-rock compositions of seawater-dominated hydrothermal alteration at the Arctic volcanogenic massive sulfide prospect, Alaska. *Econ. Geol.* **83**, 822-842.

SCHOELL, M. (1976): Heating and convection within the Atlantis II Deep geothermal system of the Red Sea. *In* Proc. Second United Nations Symposium on the Development and Use of Geothermal Resources **1**, 583-590.

——— & STAHL, W. (1972): The carbon isotopic composition and the concentration of the dissolved inorganic carbon in the Atlantis II Deep brines-Red Sea. *Earth Planet. Sci. Lett.* **15**, 206-211.

——— & FABER, E. (1978): New isotopic evidence for the origin of Red Sea brines. *Nature* **275**, 436-438.

SCHUMANN, D. (1978): *Mineralbestimmungen mit Röntgendiffractometrie an Sedimenten der Erschlamm Kampagnen VA-01 und VA-03 der Valdivia.* Ph.D. thesis, Univ. Mainz, Mainz, Federal Republic of Germany.

SEYFRIED, W.E., JR. & BISCHOFF, J.L. (1977): Hydrothermal transport of heavy metals by seawater: The role of seawater–basalt ratio. *Earth Planet. Sci. Lett.* **34**, 71-77.

——— & ——— (1981): Experimental seawater–basalt interaction at 300°C, 500 bars: Chemical exchange, secondary mineral formation and implications for the transport of heavy metals. *Geochim. Cosmochim. Acta* **45**, 135-149.

SHANKS, W.C., III (1983): Economic and exploration significance of Red Sea metalliferous brine deposits. *In* Cameron Volume On Unconventional Mineral Deposits (W.C. Shanks, III, ed.), 157-171. American Inst. Mining, Metall., and Petroleum Engineers Inc., New York.

——— & BISCHOFF, J.L. (1977): Ore transport and deposition in the Red Sea geothermal system: A geochemical model. *Geochim. Cosmochim. Acta* **41**, 1507-1519.

——— & ——— (1980): Geochemistry, sulfur isotope composition, and accumulation rates of the Red Sea geothermal deposits. *Econ. Geol.* **75**, 445-459.

———, ——— & ROSENBAUER R.J. (1981): Seawater sulfate reduction and sulfur isotope fractionation in basaltic systems: Interaction of seawater with fayalite and magnetite at 200–350°C. *Geochim. Cosmochim. Acta* **45**, 1977-1996.

——— & SEYFRIED, W.E., JR. (1987): Stable isotope studies of vent fluids and chimney minerals, southern Juan de Fuca Ridge: Sodium metasomatism and seawater sulfate reduction *J. Geophys. Res.* **92**, 11387-11399.

STOFFERS, P. & KÜHN, R. (1974): Red Sea evaporites: a petrographic and geochemical study. *Initial Reports Deep Sea Drilling Project* **23**, 821-847. U.S. Gov. Printing Office, Washington, D.C.

STYRT, M., BRACKMANN, A., HOLLAND, H., CLARK, B., PISUTHA-ARNOND, V., ELDRIDGE, C. & OHMOTO, H. (1981): The mineralogy and the isotopic composition of sulphur in hydrothermal sulphide/sulphate deposits on the East Pacific Rise, 21°N latitude. *Earth Planet. Sci. Lett.* **53**, 328-390.

TIVEY, M.K. & DELANEY, J.R. (1986): Growth of large sulfide structures on the Endeavour Segment of the Juan de Fuca Ridge. *Earth Planet. Sci. Lett.* **77**, 303-317.

TRÜPER, H.G. (1969): Bacterial sulfate reduction in the Red Sea hot brines. *In* Hot Brines and Recent Heavy Metal Deposits in the Red Sea (E.T. Degens & D.A.

Ross, eds.), 263-271. Springer-Verlag, New York.

VON DAMM, K.L., EDMOND, J.M., GRANT, B., MEASURES, C.I., WALDEN, B. & WEISS, R.F. (1985): Chemistry of submarine hydrothermal solutions at 21°N, East Pacific Rise. *Geochim. Cosmochim. Acta* **49**, 2197-2221.

WEBER-DIEFENBACH, K. (1977): Geochemistry and diagenesis of recent heavy metal ore deposits at the Atlantis II Deep (Red Sea). *In* Time and Stratabound Ore Deposits (D.D. Klemm & H.J. Schneider, eds.), 419-436. Springer-Verlag, New York.

WENNER, D.B. & TAYLOR, H.P., JR. (1971): Temperatures of serpentinization of ultramafic rocks based on O^{18}/O^{16} fractionation between coexisting serpentine and magnetite. *Contr. Mineral. Petrology* **32**, 165-185.

WOODRUFF, L.G. & SHANKS, W.C., III (1988): Sulfur isotope study of sulfide minerals and hydrothermal fluids from 21°N, East Pacific Rise: Deep sulfur sources and disequilibrium mixing. *J. Geophys. Res.* **93**, 4562-4572.

YEH, H. & SAVIN, S.M. (1977): Mechanisms of burial metamorphism of argillaceous sediments: 3. O-isotope evidence. *Geol. Soc. Amer. Bull.* **88**, 1321-1330.

ZIERENBERG, R.A. (1984): The Mattagami Lake Mine Archean Zn–Cu deposit, Quebec: Hydrothermal coprecipitation of talc and sulfides in a sea-floor brine pool–evidence from geochemistry, oxygen isotopes, and mineral chemistry – a discussion. *Econ. Geol.* **79**, 1951-1952.

_____ & SHANKS, W.C., III (1983): Mineralogy and geochemistry of epigenetic features in metalliferous sediment, Atlantis II Deep, Red Sea. *Econ. Geol.* **78**, 57-72.

_____, _____ & BISCHOFF, J.L. (1984): Massive sulfide deposits at 21°N, East Pacific Rise: Chemical composition, stable isotopes, and phase equilibria. *Geol. Soc. Amer. Bull.* **95**, 922-929.

_____ & _____ (1986): Isotopic constraints on the origin of the Atlantis II, Suakin and Valdivia brines, Red Sea. *Geochim. Cosmochim. Acta* **50**, 2205-2214.

_____, _____, SEYFRIED, W.E., JR., KOSKI, R.A. & STRICKLER, M.D. (1988): Mineralization, alteration and hydrothermal metamorphism of the ophiolite-hosted Turner–Albright sulfide deposit, southwestern Oregon. *J. Geophys. Res.* **93**, 4657-4674.

APPENDIX. ISOTOPIC AND CHEMICAL DATA FOR ATLANTIS II DEEP METALLIFEROUS SEDIMENT AND VEINS

TABLE A. EPIGENETIC VEIN PRECIPITATES

Core (depth cm)	Description	Sulfides $\delta^{34}S$	Sulfates $\delta^{34}S$	$\delta^{18}O$	Sr(ppm)	$^{87}Sr/^{86}Sr$	Carbonates, Silicates, and Oxides $\delta^{13}C$	$\delta^{18}O$	T°C	$^{87}Sr/^{86}Sr$
35 K (456-459)	Anhydrite fissure	Sp 5.3 Py 5.1±.1(2)	An 21.9±.1(3)	An 9.0	312	0.70714		Sm 10.4	163	
35 K (456-470)	Anhydrite fissure	Py 5.6±.5(3)	An 21.4±.2(3)	An 8.4	300	0.70711		Sm 11.4±.2(2)	148	
48 K (346-350)	Anhydrite vein	Py 5.8±.1(2)	An 20.9±.1(2)				-1.8	Sm 11.6±.2(2) Ms 25.9	146 54	
48 K (445-448)	Anhydrite vein	Py 4.7	An 22.3	An 7.8±.2(2)				Sm 7.9±.5(2)	208	
48 K (567-574)	Anhydrite vein		An 21.8±.1(2)	An 8.5±.1(2)	198	0.70701	-3.9	Ms 24.4	61	
52 K (149-155)	Anhydrite-silicate sulfide ooze	Py 5.9±.2(3)	An 22.3±.2(3)	An 8.4				Sm 6.8	233	
52 K (227-234)	Anhydrite fissure	Sp 4.5 Py 5.0±.1(2)	An 22.4	An 9.8	315	0.70710		Sm 5.4±.1(2)	271	
52 K (314-317)	Anhydrite fissure	Py 5.1	An 22.3	An 8.9						
52 K (356-362)	Talc vein	Sp 5.0±.1(2) Py 5.3±.3(2)		An 9.3				Sm 6.8	233	0.70732
52 K (571-574)	Talc vein	Sp 5.0±.1(2) Py 6.5±.5(2)	L 19.8	An 10.8				Ch 2.2	250	0.70735
64 K (441-495)	Anhydrite vein		An 20.8							
64 K (445-452)	Anhydrite vein	Py 10.5±.4(2)	An 22.1	An 10.3				Sm 10.4±.8(2)	163	
413 K (307-313)	Talc vein			An 10.3				Sm 8.8	190	
413 K (382-398)	Talc vein	Py 4.9±.2(2)	L 21.0	An 9.1				Sm 8.9 Sm* 7.5±.4(2)	188 216	0.70749
268 K (980-990)	Anhydrite fissures and veins	Sp 4.9±.2(5) Py 22.9	An 22.3±.2(2) Ba 22.7±.2(2)	An 8.0 Ba 8.0±.3(2)	420	0.70719				
268 K (1064-1068)	Anhydrite fissures and veins		An 22.5±.1(2)	An 10.5±.1(2)	449	0.70747				
268 K (1085-1087)	Anhydrite fissures and veins		An 22.4±.1(2)	An 9.2 f.gr. An 10.2±.2(2)	424	0.70744				
268 K (1020-1110)	Anhydrite fissures and veins		An 22.7±.1(2)	An 8.5	473	0.70746				
492 K (885)	Magnetite-hematite pyroxene	Cp 9.5	An 23.4±.1(2)	An 8.7				Sm 10.0±.3(2) Hm -4.7; Mt-5.1 Px 1.2	169	0.70635
17 P (825-850)	Magnetite-hematite pyroxene		An 21.9±.3(2)	An 8.9				Mt -3.5		0.70616
18 P (825-855)	Magnetite-hematite pyroxene							Mt -3.3		
18 P (1100-1125)	Magnetite-hematite pyroxene							Mt -3.5		
18 P (1125-1150)	Magnetite-hematite pyroxene		An 21.4±.2(2)	An 8.7				Mt -3.2 Px 0.9		0.70718

TABLE B. BRINE POOL PRECIPITATES

Core (depth cm)	Description	Sulfides	Sulfates				Carbonates and Silicates		
		$\delta^{34}S$	$\delta^{34}S$	$\delta^{18}O$	Sr(ppm)	$^{87}Sr/^{86}Sr$	$\delta^{13}C$	$\delta^{18}O$	T°C
81 BC (0-50)	Silicate ooze							Sm 15.6	99
84 BC (0-50)	Silicate ooze							Sm 16.9	87
64 K (511-515)	Anhydrite bed	Sp 2.6 Py 4.3	An 24.0±.7(2) Gy 22.9	An 8.9					
71 K (355-361)	Sulfide bed	Sp 5.5±.1(3) Py 5.7±2(2)							
71 K (366-390)	Hematite-silicate breccia			An 9.9					
71 K (1089-1095)	Hematite-silicate breccia			An 10.8					
84 K (211-216)	Anhydrite layer		An 23.1±.2(3) Ba 21.6	An 12.0			-3.8	Sm 14.6 Ms 21.4	110 82
84 K (280-286)	Anhydrite layer		An 23.3±.3(2)	An 10.7			-2.4	Sm 20.1 Ms 32.3	62 19
84 K (558-562)	Anhydrite layer		An 23.8	An 12.0					
432 K (302)	Anhydrite layer (vein?)		An 23.5				0.9	Ms 24.8	58
432 K (326-334)	Limonite-sulfide breccia			An 11.4			1.6	Ms 26.7	47
436 K (653-657)	Sulfide ooze	Py 2.5±.6(4)							
436 K (730-735)	Anhydrite nodule		An 22.9	An 11.4±.1(2)					
436 K (742-748)	Anhydrite nodule		An 23.1±.1(2)	An 12.2					
459 P (99-110)	Anhydrite bed	Py 14.0±6.6(2)	An 22.9±.2(2) Ba 21.7±.1(2)	An 11.0			0.6	Ms 25.5	54
578 P (53-57)	Anhydrite bed		An 24.5±.4(3)	An 10.7	202	0.70722			
578 P (165-170)	Anhydrite bed	Sp 3.9±.2(2) Py 4.5±.8(4)	An 23.6±.5(2)	An 11.5					
578 P (200-204)	Anhydrite bed	Py 23.4	An 25.0±.4(4)	An 11.3	323	0.70706			

Abbreviations: An = Anhydrite, Ba = barite, Ch = chlorite, Cp = Chalcopyrite, f.gr. = fine grained, Gy = gypsum, Hm = hematite, L = cold water leach sulfate, Ms = Mn-Fe carbonate, Mt = magnetite, Px = pyroxene, Sm = smectite, Sp = sphalerite.

For samples with replicate analysis value given is the mean ±.x, one standard deviation on (n) number of analyses.
*Smectite from vein selvage.